EURASIP Journal on Wireless Communications and Networking 2005:3, 308–322

Flexible Transmission Scheme for 4G Wireless Systems with Multiple Antennas

François Horlin
Wireless Research, Interuniversity Micro-Electronics Center (IMEC), Kapeldreef 75, B-3001 Leuven, Belgium
Email: francois.horlin@imec.be

Frederik Petré
Wireless Research, Interuniversity Micro-Electronics Center (IMEC), Kapeldreef 75, B-3001 Leuven, Belgium
Email: petre@imec.be

Eduardo Lopez-Estraviz
Wireless Research, Interuniversity Micro-Electronics Center (IMEC), Kapeldreef 75, B-3001 Leuven, Belgium
Email: lopezest@imec.be

Frederik Naessens
Wireless Research, Interuniversity Micro-Electronics Center (IMEC), Kapeldreef 75, B-3001 Leuven, Belgium
Email: naessen@imec.be

Liesbet Van der Perre
Wireless Research, Interuniversity Micro-Electronics Center (IMEC), Kapeldreef 75, B-3001 Leuven, Belgium
Email: vdperre@imec.be

Received 15 October 2004; Revised 11 May 2005

New air interfaces are currently being developed to meet the high requirements of the emerging wireless communication systems. In this context, the combinations of the multicarrier (MC) and spread-spectrum (SS) technologies are promising candidates. In this paper, we propose a generic transmission scheme that allows to instantiate all the combinations of orthogonal frequency-division multiplexing (OFDM) and cyclic-prefixed single-carrier (SC) modulations with direct-sequence code-division multiple access (DS-CDMA). The generic transmission scheme is extended to integrate the space-division multiplexing (SDM) and the orthogonal space-time block coding (STBC). Based on a generalized matrix model, the linear frequency-domain minimum mean square error (MMSE) joint detector is derived. A mode selection strategy for up- and downlink is advised that efficiently trades off the cost of the mobile terminal and the achieved performance of a high-mobility cellular system. It is demonstrated that an adaptive transceiver that supports the proposed communication modes is necessary to track the changing communication conditions.

Keywords and phrases: code-division multiple access, OFDM, cyclic-prefix single carrier, space-division multiplexing, space-time block coding, joint detection.

1. INTRODUCTION

Because of the limited frequency bandwidth, on the one hand, and the potential limited power of terminal stations, on the other hand, spectral and power efficiency of future systems should be as high as possible. New air interfaces need to be developed to meet the new system requirements. Combinations of the multicarrier (MC) and spread-spectrum (SS) modulations, named multicarrier spread-spectrum techniques, could be interesting candidates. They might benefit from the main advantages of both MC and SS schemes such as high spectral efficiency, multiple-access capabilities, narrowband interference rejection, simple one-tap equalization, and so forth.

Cellular systems of the third generation are based on the recently emerged direct-sequence code-division multiple-access (DS-CDMA) technique [1]. Intrinsically, DS-CDMA has interesting networking abilities. First, the

communicating users do not need to be time synchronized in the uplink. Second, soft handover is supported between two cells making use of different codes at the base stations. However, the system suffers from intersymbol interference (ISI) and multiuser interference (MUI) caused by multipath propagation, leading to a high loss of performance.

The use of the orthogonal frequency-division multiplexing (OFDM) modulation is widely envisaged for wireless local area networks [2]. At the cost of the addition of a cyclic prefix, the time dispersive channel is seen in the frequency domain as a set of parallel independent flat subchannels and can be equalized at a low-complexity. An alternative approach to OFDM, that benefits from the same low complexity equalization property, is single-carrier block transmission (SCBT), also known as single-carrier (SC) with frequency-domain equalization. Since the SCBT technique benefits from a lower peak-to-average power ratio (PAPR), [3] encourages the use of SCBT in the uplink and OFDM in the downlink in order to reduce the constraints on the analog front end and the processing complexity at the terminal.

There are potential benefits in combining OFDM (or SCBT) and DS-CDMA. Basically the frequency-selective channel is first equalized in the frequency domain using the OFDM modulation technique. DS-CDMA is applied on top of the equalized channel, keeping the interesting orthogonality properties of the codes. The DS-CDMA signals are either spread across the OFDM carriers (referred to as intrablock spreading) leading to multicarrier CDMA (MC-CDMA) [4, 5, 6, 7], or across the OFDM blocks (referred to as interblock spreading) leading to multicarrier block-spread CDMA (MCBS-CDMA) [8, 9, 10, 11]. The SCBT counterparts named here single-carrier CDMA (SC-CDMA) and single-carrier block-spread CDMA (SCBS-CDMA) have also been proposed in [12, 13, 14, 15], respectively. The different flavors to mix the MC and SS modulations complement each other and allow to make an efficient tradeoff between the spectral and power efficiency according to the user requirements, channel propagation characteristics (time and frequency selectivity), and terminal resources. For example, it has been recently proposed, in [16] for the downlink, and in [17] for the uplink, to perform a two-dimensional spreading (combination of MC-CDMA with MCBS-CDMA) in order to cope with the time and frequency selectivity of the channels. The chips of a given symbol are mapped on adjacent channels where the fading coefficients are almost constant so that the orthogonality properties of the codes are preserved and a low-complexity single-user detector can be used.

To meet the data rate and quality-of-service requirements of future broadband cellular systems, their spectral efficiency and link reliability should be considerably improved, which cannot be realized by using traditional single-antenna communication techniques. To achieve these goals, multiple-input multiple-output (MIMO) systems, which deploy multiple antennas at both ends of the wireless link, exploit the extra spatial dimension, besides the time, frequency, and code dimensions, which allows to significantly increase the spectral efficiency and/or to significantly improve the link reliability relative to single-antenna systems [18, 19, 20]. MIMO systems explicitly rely on the fact that the channels created by the additional spatial dimension are independent from each other. This is approximately true in rich scattering environments. However, when the channels are correlated, the gain obtained by the use of multiple antennas is limited. Until very recently, the main focus of MIMO research was on single-user communications over narrowband channels, thereby neglecting the multiple-access aspects and the frequency-selective fading channel effects, respectively.

First, if the multiantenna propagation channels are sufficiently uncorrelated, MIMO systems can create $N_{\min}$ parallel spatial pipes, which allows to realize an $N_{\min}$-fold capacity increase, where $N_{\min} = \min\{N_T, N_R\}$ (N_T and N_R denote the number of transmit and receive antennas, resp.) is called the spatial multiplexing gain [18, 19, 20]. Specifically, space-division multiplexing (SDM) techniques exploit this spatial multiplexing gain, by simultaneously transmitting $N_{\min}$ independent information streams at the same frequency [21, 22]. In [23], SDM is combined with SC-CDMA to increase the data rate of multiple users in a broadband cellular network.

Second, MIMO systems can also create $N_T N_R$ independently fading channels between the transmitter and the receiver, which allows to realize an $N_T N_R$-fold diversity increase, where $N_T N_R$ is called the multiantenna diversity gain. Specifically, space-time coding (STC) techniques exploit diversity and coding gains, by encoding the transmitted signals not only over the temporal domain but also over the spatial domain [24, 25, 26]. Space-time block coding (STBC) techniques, introduced in [25] for $N_T = 2$ transmit antennas, and later generalized in [26] for any number of transmit antennas, are particularly appealing because they facilitate maximum-likelihood (ML) detection with simple linear processing. However, these STBC techniques have originally been designed for frequency-flat fading channels exploiting only multiantenna diversity of order $N_T N_R$. Therefore, time-reversal (TR) STBC techniques, originally proposed in [27] for single-carrier serial transmission, have been combined with SCBT in [28, 29] for signaling over frequency-selective fading channels. In [30, 31], the TR-STBC technique of [28] is combined with SC-CDMA to improve the performance of multiple users in a broadband cellular network. Although this technique enables low-complexity chip equalization in the frequency domain, it does not preserve the orthogonality among users, and hence, still suffers from multiuser interference. The space-time coded multiuser transceiver of [32], which combines the TR-STBC technique of [29] with SCBS-CDMA, preserves the orthogonality among users as well as transmit streams, regardless of the underlying multipath channels. This allows for deterministic ML user separation through low-complexity code-matched filtering as well as deterministic ML transmit stream separation through linear processing. Another alternative to remove MUI deterministically in a space-time coded multiuser setup [33, 34] combines generalized multicarrier (GMC) CDMA, originally developed in [35], with the STBC techniques of [26] but implemented on a per-carrier basis.

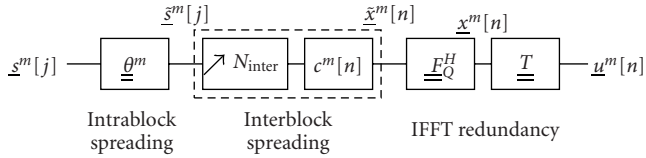

Figure 1: Single-antenna transmitter model.

We propose a transmission chain composed of generic blocks and able to instantiate all the communication modes combining OFDM/SCBT and DS-CDMA as special cases. In contrast with the transceiver proposed in [35, 36, 37] that relies on a sharing of the set of carriers to retain the orthogonality between the users, our transmission scheme relies on orthogonal CDMA, and thus inherits the nice advantages of CDMA related to universal frequency reuse in a cellular network, like increased capacity and simplified network planning. Furthermore, the focus is especially put on the communication modes emerging in the standards. We demonstrate the rewarding synergy between existing and evolving MIMO communication techniques and our generic transmission technique, which allows to increase the spectral efficiency and to improve the link reliability of multiple users in a broadband cellular network. Considering realistic propagation channels, we also advise a strategy for mode selection according to the communication conditions, making an efficient tradeoff between the desired performance and the required computational complexity.

The paper is organized as follows. In Section 2, the generic transmission scheme is presented that can capture the standard emerging communication modes as special cases. It is shown how the MC and SC modes can be instantiated. Section 3 is devoted to the extension of the transmission scheme introduced in Section 2 to multiple-antenna systems. Both SDM and STBC multiple-antenna techniques are considered. A low-complexity minimum mean square error (MMSE) receiver is designed in Section 4 based on a generalized matrix model. Finally, a strategy for communication mode selection is proposed in Section 5, based on the evaluation of the cost and performance of each mode in a highly mobile cellular environment.

In the sequel, we use single- and double-underlined letters for the vectors and matrices, respectively. Matrix $\underline{\underline{I}}_N$ is the identity matrix of size N and matrix $\underline{\underline{0}}_{M\times N}$ is a matrix of zeros of size $M \times N$. The operators $(\cdot)^*$, $(\cdot)^T$, and $(\cdot)^H$ denote, respectively, the complex conjugate, transpose, and transpose conjugate of a vector or a matrix. The operator $\otimes$ is the Kronecker product between two vectors or matrices. We index the transmitted block sequence by i, the MIMO coded block sequence and the intrablock chip block sequence by j, and the interblock chip block sequence by n.

2. SINGLE-ANTENNA GENERIC TRANSMISSION SCHEME

The transmission scheme for the mth user ($m = 1, \ldots, M$) is depicted in Figure 1. Since we focus on a single-user transmission, the transmission scheme applies to both the up- and downlink. In the uplink, the different user's signals are multiplexed at the receiver, after propagation through their respective multipath channels. In the downlink, the different user signals are multiplexed at the transmitter, before the inverse fast Fourier transform (IFFT) operation.

The transmission scheme comprises four basic operations: intrablock spreading, interblock spreading, IFFT, and adding transmit redundancy. The symbols $s^m[j]$ are first serial-to-parallel converted into blocks of B symbols, leading to the sequence $\underline{s}^m[j] := [s^m[jB] \cdots s^m[(j+1)B-1]]^T$. The blocks $\underline{s}^m[j]$ are linearly precoded with a $Q \times B$ ($Q \geq B$) matrix, $\underline{\underline{\theta}}^m$, which possibly introduces some redundancy and spreads the symbols in $\underline{s}^m[j]$ with length-Q codes as follows:

$$\underline{\tilde{s}}^m[j] := \underline{\underline{\theta}}^m \cdot \underline{s}^m[j]. \tag{1}$$

We refer to this first operation as *intrablock spreading*, since the information symbols $s^m[j]$ are spread *within* a single precoded block $\underline{\tilde{s}}^m[j]$. The precoded block sequence $\underline{\tilde{s}}^m[j]$ is then block spread with the elements $c^m[n]$ of a length-N_{inter} code sequence, leading to N_{inter} successive chip blocks:

$$\underline{\tilde{x}}^m[n] := \underline{\tilde{s}}^m[j]\, c^m[n - jN_{\text{inter}}], \tag{2}$$

where $j = \lfloor n/N_{\text{inter}} \rfloor$. We refer to this second operation as *interblock spreading*, since the information symbols $s^m[j]$ are spread *along* N_{inter} different chip blocks. The third operation involves the transformation of the frequency-domain chip block sequence $\underline{\tilde{x}}^m[n]$ into the time-domain chip block sequence:

$$\underline{x}^m[n] := \underline{\underline{F}}_Q^H \cdot \underline{\tilde{x}}^m[n], \tag{3}$$

where $\underline{\underline{F}}_Q^H$ is the $Q \times Q$ IFFT matrix. Finally, the $K \times Q$ ($K \geq Q$) transmit matrix $\underline{\underline{T}}$ possibly adds some transmit redundancy to the time-domain chip blocks:

$$\underline{u}^m[n] := \underline{\underline{T}} \cdot \underline{x}^m[n]. \tag{4}$$

With $K = Q + L$ denoting the total block length $\underline{\underline{T}} = \underline{\underline{T}}_{\text{cp}} := [\underline{\underline{I}}_{\text{cp}}^T, \underline{\underline{I}}_Q^T]^T$, where $\underline{\underline{I}}_{\text{cp}}$ consists of the last L rows of $\underline{\underline{I}}_Q$, $\underline{\underline{T}}$ adds redundancy in the form of a length-L cyclic prefix (cp). The chip block sequence $\underline{u}^m[n]$ is parallel-to-serial converted into the scalar sequence $[u^m[nK] \cdots u^m[(n+1)K-1]]^T := \underline{u}^m[n]$, and transmitted over the air at a rate $1/T_c$ (T_c stands for the chip duration).

In the following, we will detail how our generic transmission scheme instantiates different communication modes, and, thus, supports different emerging communication standards. We distinguish between the MC modes, on the one hand, and the SC modes, on the other hand. In Figure 2, the principle of CDMA spreading in two possible dimensions is illustrated.

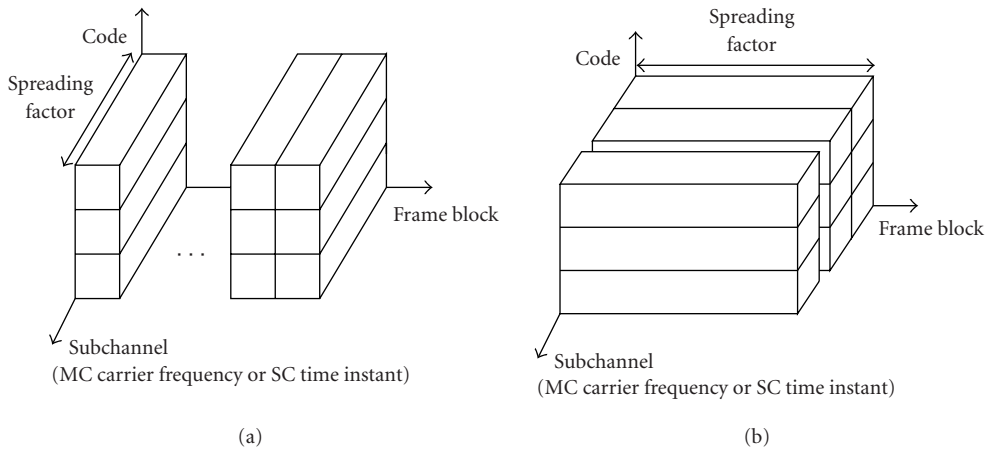

Figure 2: (a) Intrablock spreading pattern (MC/SC-CDMA). (b) Interblock spreading pattern (MCBS/SCBS-CDMA).

2.1. Instantiation of the multicarrier modes

The MC modes always comprise the IFFT operation, and add transmit redundancy in the form of a cyclic prefix ($\underline{\underline{T}} = \underline{\underline{T}}_{\text{cp}}$). The MC modes comprise MC-CDMA and MCBS-CDMA as particular instantiations of the generic transmission scheme.

2.1.1. MC-CDMA

As we have indicated in the introduction, MC-CDMA first performs classical DS-CDMA symbol spreading, followed by OFDM modulation, such that the information symbols are spread across the different subcarriers located at different frequencies and characterized by a different fading coefficient [4, 5, 6]. With $Q = BN_{\text{intra}}$ and N_{intra} the intrablock spreading code length, the $Q \times B$ intrablock spreading matrix $\underline{\underline{\theta}}^m = \underline{\underline{\beta}}^m$ spreads the chips across the subcarriers, where the mth user's $Q \times B$ spreading matrix $\underline{\underline{\beta}}^m$ is defined as

$$\underline{\underline{\beta}}^m := \underline{\underline{I}}_B \otimes \underline{a}^m, \tag{5}$$

with $\underline{a}^m := [a^m[0] \cdots a^m[N_{\text{intra}} - 1]]^T$ the mth user's $N_{\text{intra}} \times 1$ code vector. The interblock spreading operation is discarded by setting $N_{\text{inter}} = 1$. Since intrablock spreading does not preserve the orthogonality among users in a frequency-selective channel, MC-CDMA requires advanced multiuser detection for uplink reception in the base station, and frequency-domain chip equalization for downlink reception in the mobile station. MC-CDMA has been proposed as a candidate air interface for future broadband cellular systems [7].

2.1.2. MCBS-CDMA

The MCBS-CDMA transmission scheme is the only MC mode that comprises the interblock spreading operation $N_{\text{inter}} > 1$. Since the CDMA spreading is applied on each carrier independently, which can be seen as a constant fading channel if the propagation environment is static, MCBS-CDMA retains the orthogonality among users in both up- and downlink [11]. Hence, it has the potential to convert a difficult multiuser detection problem into an equivalent set of simpler and independent single-user equalization problems. However, it will be shown in Section 5 that the performance of MCBS-CDMA is highly degraded under medium-to-high mobility conditions since the orthogonality between the users is lost in that case. In case no channel state information (CSI) is available at the transmitter, it performs linear precoding to robustify the transmitted signal against frequency-selective fading. In case CSI is available at the transmitter, it allows to optimize the transmit spectrum of each user separately through adaptive power and bit loading. Note that classical MC-DS-CDMA can be seen as a special case of MCBS-CDMA, because it does not include linear precoding, but, instead, only relies on bandwidth-consuming forward error correction (FEC) coding to enable frequency diversity [8, 10, 38].

2.2. Instantiation of the single-carrier modes

The SC modes employ a fast Fourier transform (FFT) as part of the intrablock spreading operation to annihilate the IFFT operation. For implementation purposes, however, the IFFT is simply removed (and not compensated by an FFT), in order to minimize the implementation complexity. The SC modes rely on cyclic prefixing ($\underline{\underline{T}} = \underline{\underline{T}}_{\text{cp}}$) to make the channel appear circulant. The SC modes comprise SC-CDMA and SCBS-CDMA as particular instantiations of the generic transmission scheme.

2.2.1. SC-CDMA

The SC-CDMA transmission scheme, which combines SCBT with DS-CDMA, can be interpreted as the SC counterpart of MC-CDMA [12, 13]. This mode is captured through our general transmission scheme, by setting $Q = BN_{\text{intra}}$. The intrablock spreading matrix $\underline{\underline{\theta}}^m = \underline{\underline{F}}_Q \cdot \underline{\underline{\beta}}^m$, with $\underline{\underline{\beta}}^m$ defined in (5), performs symbol spreading on the B information symbols, followed by an FFT operation to compensate

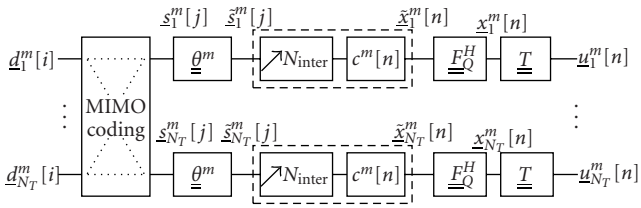

Figure 3: MIMO transmitter model.

for the subsequent IFFT operation. Like MC-CDMA, SC-CDMA does not preserve the orthogonality among the users in a frequency-selective channel. It requires advanced multiuser detection for uplink reception at the base station and chip equalization for downlink reception at the mobile terminal. On the contrary to MC-CDMA, each user symbol is spread amongst multiple subchannels of the same power attenuation. The interblock spreading operation is left out by setting $N_{\text{inter}} = 1$.

2.2.2. SCBS-CDMA

The SCBS-CDMA transceiver can be considered as the SC counterpart of MCBS-CDMA. It is the only SC mode that entails the interblock spreading operation ($N_{\text{inter}} > 1$). The intrablock spreading matrix $\underline{\underline{\theta}}^m = \underline{\underline{F}}_Q$ only performs an FFT operation to compensate for the subsequent IFFT operation. If the propagation channels are static, SCBS-CDMA retains the orthogonality among users in both the up- and downlink, even after propagation through a frequency-selective channel (like MCBS-CDMA). It also converts a difficult multiuser detection problem into an equivalent set of simpler and independent single-user equalization problems. The orthogonality property is however lost in time-selective channels, as studied numerically in Section 5.

3. EXTENSION TO MULTIPLE ANTENNAS

The generic transmission model is extended in Figure 3 to include two types of MIMO techniques. We assume N_T antennas at the transmit side and N_R antennas at the receive side. The information symbols $d^m_{n_T}[i]$, which are assumed independent and of variance equal to σ_d^2, are first serial-to-parallel converted into blocks of B symbols, leading to the block sequence $\underline{d}^m_{n_T}[i] := [d^m_{n_T}[iB] \cdots d^m_{n_T}[(i+1)B-1]]^T$ for $n_T = 1, \ldots, N_T$. A MIMO coding operation is performed across the different transmit antenna streams, that results into the N_T antenna sequences $\underline{s}^m_{n_T}[j]$ input to the generic transmission scheme. The overall rate increase obtained by the use of multiple antennas is either 1 or N_T depending on the MIMO technique that is selected.

3.1. Space-division multiplexing

In this section, we combine our generic transmission scheme with SDM, which allows to instantiate all combinations of SDM with OFDM/SCBT and CDMA as special cases. The SDM technique is implemented by sending independent streams on each transmit antenna n_T, as expressed in

$$\underline{s}^m_{n_T}[j] = \underline{d}^m_{n_T}[i], \tag{6}$$

where $j = i$.

3.2. Space-time block coding

In this section, we combine our generic transmission scheme with STBC, which allows to instantiate all combinations of STBC with OFDM/SCBT and CDMA as special cases. For conciseness, we limit ourselves to the case of $N_T = 2$ transmit antennas (Alamouti scheme [25, 27]). The STBC coding is implemented by coding the two antenna streams across two time instants, as expressed in

$$\begin{bmatrix} \underline{s}^m_1[j] \\ \underline{s}^m_2[j] \end{bmatrix} = \begin{bmatrix} \underline{d}^m_1[i] \\ \underline{d}^m_2[i] \end{bmatrix}, \qquad \begin{bmatrix} \underline{s}^m_1[j+1] \\ \underline{s}^m_2[j+1] \end{bmatrix} = \underline{\underline{\chi}} \cdot \begin{bmatrix} \underline{d}^m_1[i]^* \\ \underline{d}^m_2[i]^* \end{bmatrix}, \tag{7}$$

where $i = \lfloor j/2 \rfloor$ and

$$\underline{\underline{\chi}} := \underline{\underline{\chi}}_{N_T} \otimes \underline{\underline{\chi}}_B \quad \text{with } \underline{\underline{\chi}}_{N_T} := \begin{bmatrix} 0 & -1 \\ 1 & 0 \end{bmatrix}. \tag{8}$$

In the case of the MC modes, the STBC coding is applied in the frequency domain on a per-carrier basis so that

$$\underline{\underline{\chi}}_B := \underline{\underline{I}}_B. \tag{9}$$

In the case of the SC modes, the STBC coding is applied in the time domain by further permuting the vector elements so that

$$\underline{\underline{\chi}}_B := \underline{\underline{F}}_B^T \cdot \underline{\underline{F}}_B \tag{10}$$

is a $B \times B$ permutation matrix implementing a time reversal.

It is easily checked that the transmitted block at time instant $j+1$ from one antenna is the time-reversed conjugate of the transmitted symbol at time instant j from the other antenna (with possible permutation and sign change). As we will show later, this property allows the deterministic transmit stream separation at the receiver, regardless of the underlying frequency-selective channels.

4. RECEIVER DESIGN

4.1. Cyclostationarization of the channels

Adopting a discrete-time baseband equivalent model, the chip-sampled received signal at antenna n_R ($n_R = 1, \ldots, N_R$), $v_{n_R}[n]$, is the superposition of a channel-distorted version of the MN_T transmitted user signals, which can be written as

$$v_{n_R}[n] = \sum_{m=1}^{M} \sum_{n_T=1}^{N_T} \sum_{l=0}^{L^m} h^m_{n_R,n_T}[l] u^m_{n_T}[n-l] + w_{n_R}[n], \tag{11}$$

where $h^m_{n_R,n_T}[l]$ is the chip-sampled finite impulse response (FIR) channel of order L^m that models the frequency-selective multipath propagation between the mth user's antenna n_T and the base station antenna n_R, including the effect of transmit/receive filters and the remaining asynchronism of the quasisynchronous users, and $w_{n_R}[n]$ is additive white Gaussian noise (AWGN) at the base station antenna n_R with variance σ_w^2. Furthermore, the maximum channel order L, that is, $L = \max_m\{L^m\}$, can be well approximated by $L \approx \lfloor(\tau_{\max,a} + \tau_{\max,s})/T_c\rfloor + 1$, where $\tau_{\max,a}$ is the maximum asynchronism between the nearest and the farthest user of the cell, and $\tau_{\max,s}$ is the maximum excess delay within the given propagation environment [35].

Assuming perfect time and frequency synchronization, the sequence $v_{n_R}[n]$ is serial-to-parallel converted into the sequence $\underline{v}_{n_R}[n] := [v_{n_R}[nK]\cdots v_{n_R}[(n+1)K-1]]^T$. From the scalar input/output relationship in (11), we can derive the corresponding block input/output relationship:

$$\underline{v}_{n_R}[n] = \sum_{m=1}^{M}\sum_{n_T=1}^{N_T}\Big(\underline{\underline{H}}^m_{n_R,n_T}[0]\cdot\underline{u}^m_{n_T}[n] + \underline{\underline{H}}^m_{n_R,n_T}[1]\cdot\underline{u}^m_{n_T}[n-1]\Big) + \underline{w}_{n_R}[n], \tag{12}$$

where $\underline{w}_{n_R}[n] := [w_{n_R}[nK]\cdots w_{n_R}[(n+1)K-1]]^T$ is the corresponding noise block sequence, $\underline{\underline{H}}^m_{n_R,n_T}[0]$ is a $K\times K$ lower triangular Toeplitz matrix with entries $[\underline{\underline{H}}^m_{n_R,n_T}[0]]_{p,q} = h^m_{n_R,n_T}[p-q]$ for $p-q\in[0,L^m]$ and $[\underline{\underline{H}}^m_{n_R,n_T}[0]]_{p,q} = 0$ else, and $\underline{\underline{H}}^m_{n_R,n_T}[1]$ is a $K\times K$ upper triangular Toeplitz matrix with entries $[\underline{\underline{H}}^m_{n_R,n_T}[1]]_{p,q} = h^m_{n_R,n_T}[K+p-q]$ for $K+p-q\in[0,L^m]$ and $[\underline{\underline{H}}^m_{n_R,n_T}[1]]_{p,q} = 0$ else (see, e.g., [35] for a detailed derivation of the single-user case). The delay-dispersive nature of multipath propagation gives rise to so-called interblock interference (IBI) between successive blocks, which is modeled by the second term in (12).

The $Q\times K$ receive matrix $\underline{\underline{R}}$ removes the redundancy from the chip blocks, that is, $\underline{y}_{n_R}[n] := \underline{\underline{R}}\cdot\underline{v}_{n_R}[n]$. With $\underline{\underline{R}} = \underline{\underline{R}}_{\text{cp}} = [\underline{\underline{0}}_{Q\times L}, \underline{\underline{I}}_Q]$, $\underline{\underline{R}}$ again discards the length-L cyclic prefix. The purpose of the transmit/receive pair is twofold. First, it allows for simple block-by-block processing by removing the IBI, that is, $\underline{\underline{R}}\cdot\underline{\underline{H}}^m_{n_R,n_T}[1]\cdot\underline{\underline{T}} = \underline{\underline{0}}_{Q\times Q}$, provided the CP length to be at least the maximum channel order L. Second, it enables low-complexity frequency-domain processing by making the linear channel convolution to appear circulant to the received block. This results in a simplified block input/output relationship in the time domain:

$$\underline{y}_{n_R}[n] = \sum_{m=1}^{M}\sum_{n_T=1}^{N_T}\dot{\underline{\underline{H}}}^m_{n_R,n_T}\cdot\underline{x}^m_{n_T}[n] + \underline{z}_{n_R}[n], \tag{13}$$

where $\dot{\underline{\underline{H}}}^m_{n_R,n_T} = \underline{\underline{R}}\cdot\underline{\underline{H}}^m_{n_R,n_T}[0]\cdot\underline{\underline{T}}$ is a circulant channel matrix, and $\underline{z}_{n_R}[n] = \underline{\underline{R}}\cdot\underline{w}_{n_R}[n]$ is the corresponding noise block sequence. Note that circulant matrices can be diagonalized by FFT operations, that is, $\dot{\underline{\underline{H}}}^m_{n_R,n_T} = \underline{\underline{F}}^H_Q\cdot\underline{\underline{\Lambda}}^m_{n_R,n_T}\cdot\underline{\underline{F}}_Q$, where $\underline{\underline{\Lambda}}^m_{n_R,n_T}$ is a diagonal matrix composed of the frequency-domain channel response between the mth user's antenna n_T and the base station antenna n_R.

4.2. Matrix model

Based on (13), a generalized matrix model is developed that relates the vector of transmitted user's symbols to the vector of received samples. It encompasses all the combinations of OFDM/SCBT with CDMA considered in this paper as special cases. Based on this model, a multiuser joint detector optimized according to the MMSE criterion will be derived and its complexity will be reduced by exploiting the cyclostationarity properties of the matrices.

The generalized input/output matrix model that relates the MIMO-coded symbol vector defined as

$$\bar{\underline{s}}[j] := \left[\bar{\underline{s}}^1[j]^T \ \cdots\ \bar{\underline{s}}^M[j]^T\right]^T \tag{14}$$

with

$$\bar{\underline{s}}^m[j] := \left[\underline{s}^m_1[j]^T \ \cdots\ \underline{s}^m_{N_T}[j]^T\right]^T \tag{15}$$

for $m = 1,\ldots,M$ to the received and noise vectors defined as

$$\begin{aligned}\bar{\underline{y}}[j] &:= \left[\bar{\underline{y}}_1[j]^T \ \cdots\ \bar{\underline{y}}_{N_R}[j]^T\right]^T,\\ \bar{\underline{z}}[j] &:= \left[\bar{\underline{z}}_1[j]^T \ \cdots\ \bar{\underline{z}}_{N_R}[j]^T\right]^T\end{aligned} \tag{16}$$

with

$$\begin{aligned}\bar{\underline{y}}_{n_R}[j] &:= \left[\left(\underline{y}_{n_R}[jN_{\text{inter}}]\right)^T \ \cdots\ \left(\underline{y}_{n_R}[(j+1)N_{\text{inter}}-1]\right)^T\right]^T,\\ \bar{\underline{z}}_{n_R}[j] &:= \left[\left(\underline{z}_{n_R}[jN_{\text{inter}}]\right)^T \ \cdots\ \left(\underline{z}_{n_R}[(j+1)N_{\text{inter}}-1]\right)^T\right]^T,\end{aligned} \tag{17}$$

for $n_R = 1,\ldots,N_R$, is given by

$$\bar{\underline{y}}[j] = \underline{\underline{C}}\cdot\underline{\underline{F}}^H\cdot\underline{\underline{\Lambda}}\cdot\underline{\underline{\theta}}\cdot\bar{\underline{s}}[j] + \bar{\underline{z}}[j], \tag{18}$$

where the channel matrix is defined as

$$\underline{\underline{\Lambda}} := \begin{bmatrix} \underline{\underline{\Lambda}}^1_1 & \cdots & \underline{\underline{0}}_{Q\times Q}\\ \vdots & \ddots & \vdots\\ \underline{\underline{0}}_{Q\times Q} & \cdots & \underline{\underline{\Lambda}}^M_1\\ \vdots & \vdots & \vdots\\ \underline{\underline{\Lambda}}^1_{N_R} & \cdots & \underline{\underline{0}}_{Q\times Q}\\ \vdots & \ddots & \vdots\\ \underline{\underline{0}}_{Q\times Q} & \cdots & \underline{\underline{\Lambda}}^M_{N_R}\end{bmatrix} \tag{19}$$

with

$$\underline{\underline{\Lambda}}^m_{n_R} := \left[\underline{\underline{\Lambda}}^m_{n_R,1}\cdots\underline{\underline{\Lambda}}^m_{n_R,N_T}\right] \tag{20}$$

for $m = 1,\ldots,M$ and $n_R = 1,\ldots,N_R$, and the intrablock spreading, Fourier, and interblock spreading matrices are defined, respectively, as

$$\begin{aligned}\underline{\underline{\theta}} &:= \begin{bmatrix} \underline{\underline{I}}_{N_T} \otimes \underline{\underline{\theta}}^1 & \cdots & \underline{\underline{0}}_{N_T Q \times N_T B} \\ \vdots & \ddots & \vdots \\ \underline{\underline{0}}_{N_T Q \times N_T B} & \cdots & \underline{\underline{I}}_{N_T} \otimes \underline{\underline{\theta}}^M \end{bmatrix}, \\ \underline{\underline{F}} &:= \underline{\underline{I}}_{N_R M} \otimes \underline{\underline{F}}_Q, \\ \underline{\underline{C}} &:= \underline{\underline{I}}_{N_R} \otimes \left[\underline{\underline{C}}^1 \cdots \underline{\underline{C}}^M\right], \end{aligned} \tag{21}$$

in which

$$\underline{\underline{C}}^m := \underline{c}^m \otimes \underline{\underline{I}}_Q, \tag{22}$$

with $\underline{c}^m := [c^m[0] \cdots c^m[N_{\text{inter}} - 1]]^T$. Note that the model (18) only holds for static channels. In case of time-selective channels, the channel matrices $\dot{\underline{\underline{H}}}^m_{n_R,n_T}$ cannot be diagonalized anymore and are different from one chip block to the next one.

4.2.1. Space-division multiplexing

Taking (6) into account, the model (18) is instantiated to the SDM input/output matrix model

$$\begin{aligned}\bar{\underline{y}}_{\text{sdm}}[i] = \underline{\underline{C}}_{\text{sdm}} \cdot \left(\underline{\underline{F}}_{\text{sdm}}\right)^H \cdot \underline{\underline{\Lambda}}_{\text{sdm}} \cdot \underline{\underline{\theta}}_{\text{sdm}} \cdot \underline{\underline{\chi}}_{\text{sdm}} \cdot \bar{\underline{d}}[i] \\ + \bar{\underline{z}}_{\text{sdm}}[i], \end{aligned} \tag{23}$$

where the vector of transmitted symbols is defined as

$$\bar{\underline{d}}[i] := \left[\bar{\underline{d}}^1[i]^T \cdots \bar{\underline{d}}^M[i]^T\right]^T, \tag{24}$$

with

$$\bar{\underline{d}}^m[i] := \left[\underline{d}^m_1[i]^T \cdots \underline{d}^m_{N_T}[i]^T\right]^T \tag{25}$$

for $m = 1,\ldots,M$, and the received and noise vectors are defined as

$$\begin{aligned}\bar{\underline{y}}_{\text{sdm}}[i] &:= \underline{y}[j], \\ \bar{\underline{z}}_{\text{sdm}}[i] &:= \underline{z}[j]. \end{aligned} \tag{26}$$

The MIMO encoding, intrablock spreading, channel, Fourier, and interblock spreading matrices are, respectively, given by

$$\begin{aligned}\underline{\underline{\chi}}_{\text{sdm}} &:= \underline{\underline{I}}_{MN_T B}, \\ \underline{\underline{\theta}}_{\text{sdm}} &:= \underline{\underline{\theta}}, \\ \underline{\underline{\Lambda}}_{\text{sdm}} &:= \underline{\underline{\Lambda}}, \\ \underline{\underline{F}}_{\text{sdm}} &:= \underline{\underline{F}}, \\ \underline{\underline{C}}_{\text{sdm}} &:= \underline{\underline{C}}. \end{aligned} \tag{27}$$

4.2.2. Space-time block coding

Taking (7) into account, the model (18) is instantiated to the STBC input/output matrix model

$$\begin{aligned}\bar{\underline{y}}_{\text{stbc}}[i] = \underline{\underline{C}}_{\text{stbc}} \cdot \left(\underline{\underline{F}}_{\text{stbc}}\right)^H \cdot \underline{\underline{\Lambda}}_{\text{stbc}} \cdot \underline{\underline{\theta}}_{\text{stbc}} \cdot \underline{\underline{\chi}}_{\text{stbc}} \cdot \bar{\underline{d}}[i] \\ + \bar{\underline{z}}_{\text{stbc}}[i], \end{aligned} \tag{28}$$

where the vector of transmitted symbols is given in (25) assuming that $N_T = 2$, the received and noise vectors are defined as

$$\begin{aligned}\bar{\underline{y}}_{\text{stbc}}[i] &:= \begin{bmatrix} \underline{y}[j] \\ \underline{y}[j+1]^* \end{bmatrix}, \\ \bar{\underline{z}}_{\text{stbc}}[i] &:= \begin{bmatrix} \underline{z}[j] \\ \underline{z}[j+1]^* \end{bmatrix}. \end{aligned} \tag{29}$$

The MIMO encoding, intrablock spreading, channel, Fourier, and interblock spreading matrices are, respectively, given by

$$\begin{aligned}\underline{\underline{\chi}}_{\text{stbc}} &:= \begin{bmatrix} \underline{\underline{I}}_{MN_T B} \\ \underline{\underline{I}}_M \otimes \underline{\underline{\chi}} \end{bmatrix}, \\ \underline{\underline{\theta}}_{\text{stbc}} &:= \begin{bmatrix} \underline{\underline{\theta}} & \underline{\underline{0}}_{MN_T Q \times MN_T B} \\ \underline{\underline{0}}_{MN_T Q \times MN_T B} & \underline{\underline{\theta}}^* \end{bmatrix}, \\ \underline{\underline{\Lambda}}_{\text{stbc}} &:= \begin{bmatrix} \underline{\underline{\Lambda}} & \underline{\underline{0}}_{N_R MQ \times MN_T Q} \\ \underline{\underline{0}}_{N_R MQ \times MN_T Q} & \underline{\underline{\Lambda}}^* \end{bmatrix}, \\ \underline{\underline{F}}_{\text{stbc}} &:= \begin{bmatrix} \underline{\underline{F}} & \underline{\underline{0}}_{N_R MQ \times N_R MQ} \\ \underline{\underline{0}}_{N_R MQ \times N_R MQ} & \underline{\underline{F}}^* \end{bmatrix}, \\ \underline{\underline{C}}_{\text{stbc}} &:= \begin{bmatrix} \underline{\underline{C}} & \underline{\underline{0}}_{N_R N_{\text{inter}} Q \times N_R MQ} \\ \underline{\underline{0}}_{N_R N_{\text{inter}} Q \times N_R MQ} & \underline{\underline{C}}^* \end{bmatrix}. \end{aligned} \tag{30}$$

4.3. Multiuser joint detector

In order to detect the transmitted symbol block of the pth user $\bar{\underline{d}}^p[i]$ based on the received sequence of blocks within the received vector $\bar{\underline{y}}_{\text{mode}}[i]$ ("mode" stands for "sdm" or "stbc"), a first solution consists of using a single-user receiver that inverts successively the channel and all the operations performed at the transmitter. The single-user receiver relies implicitly on the fact that CDMA spreading has been applied on top of a channel equalized in the frequency domain. After CDMA despreading, each user stream is handled independently. However the single-user receiver fails in the uplink where multiple channels have to be inverted at the same time.

The optimal solution is to jointly detect the transmitted symbol blocks of the different users within the transmitted vector $\bar{\underline{d}}[i]$ based on the received sequence of blocks within the received vector $\bar{\underline{y}}_{\text{mode}}[i]$. The optimum linear joint detector according to the MMSE criterion is computed in [39]. At the output of the MMSE multiuser detector, the estimate of

the transmitted vector is

$$\underline{\hat{d}}[i] = \left(\frac{\sigma_w^2}{\sigma_d^2}\underline{\underline{I}}_{MN_TB} + \underline{\underline{G}}_{\text{mode}}^H \cdot \underline{\underline{G}}_{\text{mode}}\right)^{-1} \cdot \underline{\underline{G}}_{\text{mode}}^H \cdot \underline{\tilde{y}}_{\text{mode}}[i], \tag{31}$$

where

$$\underline{\underline{G}}_{\text{mode}} := \underline{\underline{C}}_{\text{mode}} \cdot \left(\underline{\underline{F}}_{\text{mode}}\right)^H \cdot \underline{\underline{\Lambda}}_{\text{mode}} \cdot \underline{\underline{\theta}}_{\text{mode}} \cdot \underline{\underline{\chi}}_{\text{mode}}. \tag{32}$$

The MMSE linear joint detector consists of two main operations [39, 40].

(i) First, a filter matched to the composite impulse responses multiplies the received vector in order to minimize the impact of the white noise. The matched filter consists of the CDMA interblock despreading, the FFT operator to move to the frequency domain, the maximum ratio combining (MRC) of the different received antenna channels, the CDMA intrablock despreading, the IFFT to go back to the time domain in case of the SC modes, and the STBC decoding.

(ii) Second, the output of the matched filter is still multiplied with the inverse of the composite impulse response autocorrelation matrix of size MN_TB that mitigates the remaining intersymbol, interuser, and interantenna interference.

In the case of interblock spreading (MCBS and SCBS-CDMA), the spreading matrix $\underline{\underline{C}}$ has the property that $\underline{\underline{C}}^H\underline{\underline{C}} = \underline{\underline{I}}_{N_RQM}$ if the CDMA codes are chosen orthogonal. When the propagation channels are static, the different user streams are perfectly separated at the output of the interblock despreading operation and further treated independently. The MMSE multiuser joint detector exactly reduces to independent single-user detectors. In case of time-varying propagation channels, model (18) is not valid anymore and the multiuser MMSE joint detector cannot be simplified to single-user detectors.

In the case of intrablock spreading (MC- and SC-CDMA), however, the linear MMSE receiver is different from the single-user receiver, and suffers from a higher computational complexity. Fortunately, both the initialization complexity, which is required to compute the MMSE receiver, and the data processing complexity can be significantly reduced for MC- and SC-CDMA, by exploiting the initial cyclostationarity property of the channels. Based on a few permutations and on the properties of the block circulant matrices given in [12], it can be shown that the initial inversion of the square autocorrelation matrix of size MN_TB can be replaced by the inversion of B square autocorrelation matrices of size MN_T.

5. MODE SELECTION STRATEGY

In this section, a cost and performance comparison between the different communication modes is made, which can serve as an input for an efficient mode selection strategy.

5.1. Complexity

To evaluate the complexity of the different receivers, we distinguish between the initialization phase, when the receiver is calculated, and the data processing phase, when the received data is actually processed. The rate of the former is related to the channel's fading rate, whereas the latter is executed continuously at the symbol block rate. The complexity will be described in terms of *complex* multiply/accumulate cycle (MAC) operations. It is assumed that $2N^3$ complex MAC operations are required to invert a matrix of size N, and that $N\log_2(N)$ complex MAC operations are required to compute an FFT of size N.

5.1.1. Initialization complexity

The complexity required to compute the MMSE receiver is given in Table 1 for the base station and for the terminal, respectively. It has been assumed that the inversion of the MMSE equalizer block diagonal inner matrix is dominant. Since the size of each block is equal to the number of interfering users times the number of interfering antennas, the computation of the equalizer is more complex in case of intrablock spreading (number of interfering users equal to the number of users) than in case of interblock spreading (number of interfering users equal to one), and in case of SDM (number of interfering antennas equal to the number of transmit antennas) than in case of STBC (number of interfering antennas equal to one).

5.1.2. Data processing complexity

The complexity needed during the data processing phase to transmit and receive each user's transmitted complex symbol is further given in the Table 2. The computational effort is almost equally shared between the transmitter and the receiver in the case of the MC-based modes. In the case of the SC-based modes, all the computational effort has been moved to the receiver. From a terminal complexity point of view, it is clearly advantageous to use the SC-based modes in uplink and the MC-based modes in downlink. Both the transmission and the reception are less complex in case of interblock spreading than in case of intrablock spreading, because the (I) FFT operators can be executed at a lower rate in the former case (namely, before the spreading at the transmitter and after the despreading at the receiver). Since STBC combines N_T successive symbol blocks, it is on the overall more complex than the SDM scheme.

5.2. Peak-to-average power ratio

The PAPR is illustrated in Figure 4 for each mode as a function of the spreading factor. The user signals are spread by periodic Walsh-Hadamard codes for spreading, which are overlaid with an aperiodic Gold code for scrambling. QPSK modulation is assumed with $Q = 128$ subchannels, and a cyclic prefix length of $L = 32$. The PAPR is defined as the maximum instantaneous peak power over all combinations of the transmitted symbols divided by the average transmit power.

While the MC-based communication modes feature a very large PAPR, the SC-based communication modes have

Table 1: Initialization complexity, M users, N_T transmit antennas, Q carriers/subchannels, and B complex symbols per block.

	Base station		Mobile terminal	
	SDM	STBC	SDM	STBC
MC/SCBS-CDMA	$2QM(N_T)^3$	$2MQ$	$2Q(N_T)^3$	$2Q$
MC/SC-CDMA	$2B(MN_T)^3$	$2B(M)^3$	$2B(MN_T)^3$	$2B(M)^3$

Table 2: Data processing complexity, M users ($M = 1$ at the terminal), N_T transmit antennas, N_R receive antennas, Q carriers/subchannels, B complex symbols per block.

	Transmitter		Receiver	
	SDM	STBC	SDM	STBC
MCBS-CDMA	$\log_2 Q$	$N_T \log_2 Q$	$\frac{N_R}{N_T}\log_2 Q + N_R$	$N_R \log_2 Q + N_T N_R$
SCBS-CDMA	0	0	$\left(\frac{N_R}{N_T}+1\right)\log_2 Q + N_R$	$(N_R+1)\log_2 Q + N_T N_R$
MC-CDMA	$\frac{Q}{MB}\log_2 Q$	$N_T\frac{Q}{MB}\log_2 Q$	$\frac{N_R}{N_T}\frac{Q}{MB}\log_2 Q + N_R\frac{Q}{B}$	$N_R\frac{Q}{MB}\log_2 Q + N_T N_R\frac{Q}{B}$
SC-CDMA	0	0	$\left(\frac{N_R}{N_T}\frac{Q}{MB}+1\right)\log_2 B + N_R\frac{Q}{B}$	$\left(N_R\frac{Q}{MB}+1\right)\log_2 B + N_T N_R\frac{Q}{B}$

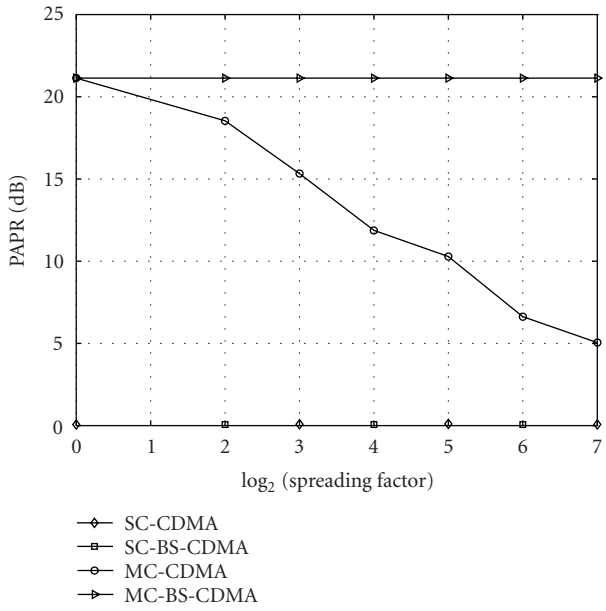

Figure 4: PAPR as a function of the spreading factor, QPSK, 128 carriers.

a PAPR close to 0 dB. MC-CDMA has a PAPR improving for an increasing spreading factor due to the fact that the total number of possible chip combinations at the output of the spreading operation is decreasing. The use of the SC-based communication modes is encouraged in the uplink to reduce the power amplifier backoff at the mobile terminal and, thus, to increase its power efficiency (even if the power amplifier backoff is not directly settled based on the low probability power peak values in the MC-based systems, it is expected that the variation in instantaneous transmitted power is much lower in the SC-based systems).

5.3. Goodput performance

We consider a mobile cellular system which operates in an outdoor suburban macrocell propagation environment. The channel model is largely inspired from the 3 GPP TR25.996 geometrical spatial channel model [41]. The radius of the cell is equal to 3 km. The mobile terminals are moving at a speed ranging from 0 (static) to 250 km/h (highly mobile). The system operates at a carrier frequency of 2 GHz, with a system bandwidth of 5 MHz. Linear antenna arrays are assumed at the mobile terminals and at the base station. An antenna spacing equal to 0.5 wavelength is selected at the mobile terminals, which results in a correlation equal to 0.2 between the antennas, and an antenna spacing equal to 5 wavelengths is selected at the base station, which results in a correlation smaller than 0.1 between the antennas. We assume a six-sector antenna at the base station and omnidirectional antennas at the mobile terminals. The propagation environment is characterized by a specular multipath composed of 6 paths (each path represents the reflection on a scatterer) and 10 subpaths per path (each subpath represents the reflection on a specific part of the scatterer). For each path, the excess delay standard deviation is equal to 238 nanoseconds, the angle spread standard deviation at the base station and that at the mobile terminals are equal to 6 and 68 degrees, respectively. For each subpath, the angle spread standard variation at the base station and that at the mobile terminals are equal to 2 and 5 degrees, respectively. The computation of the path loss is based on the COST231 Hata urban propagation model.

Monte Carlo simulations have been performed to average the bit error rate (BER) over 500 stochastic channel realizations, and to compute the corresponding goodput, defined as the throughput offered to the user assuming a retransmission of the erroneous packets until they are correctly

received. The information bandwidth is spread by the spreading factor equal to 8. The user signals are spread by periodic Walsh-Hadamard codes for spreading, which are overlaid with an aperiodic Gold code for scrambling. QPSK, 16-QAM, or 64-QAM modulation is used with $Q = 128$ subchannels, and a CP length of $L = 32$. We assume a packet size of 512 complex symbols (4 blocks of 128 symbols in case of MCBS/SCBS-CDMA or 32 blocks of 16 symbols in case of MC/SC-CDMA). Convolutional channel coding in conjunction with frequency-domain interleaving is employed according to the IEEE 802.11a/g standard. The code rate varies from 1/2, 2/3, to 3/4. At the receiver, soft-decision Viterbi decoding is used.

We distinguish between the uplink and the downlink. In the uplink, transmit power control is applied such that the received symbol energy is constant for all users. The power transmitted by each terminal depends on the actual channel experienced by it. The BER (or the goodput) is determined as a function of the received bit energy, or, equivalently, as a function of the transmit power averaged over the different channel realizations. In the downlink, no transmit power control is applied. For a constant transmit power at the base station, the received symbol energy at each terminal depends on the channel under consideration. The BER (or the goodput) is determined as a function of the transmit power, or, equivalently, as a function of the received bit energy averaged over the channel realizations. For a given received symbol energy, the required transmit powers for the different communication modes appear to be very similar.

Rather than comparing all possible modes for the two link directions, we only consider the relevant modes for each direction. For the uplink, the SC modes demonstrate two pronounced advantages compared to MC modes [3]. First, the SC modes exhibit a smaller PAPR than the MC modes, which leads to increased terminal power efficiency. Second, the SC modes allow to move the IFFT at the transmitter to the receiver, which results in reduced terminal complexity. For the downlink, the MC modes are the preferred modulation schemes, since they only incur a single FFT operation at the receiver side which also leads to reduced terminal complexity.

Figure 5 illustrates the user's goodput in the downlink of a MCBS-CDMA-based static communication system for different combinations of the constellation size and channel coding rate. The signal is received at the terminal through 2 antennas. A typical user's load of 5 users has been assumed. Looking to those combinations that give the same asymptotic goodput (16-QAM and CR 3/4 compared to 64-QAM and CR 1/2), it is always preferable to combine a high constellation size with a low code rate. The same conclusion holds in order to select the combination constellation-coding rate that maximizes the goodput for each SNR value. The envelope is obtained by progressively employing QPSK, 16-QAM, 64-QAM constellations and a code rate equal to 1/2, and then by increasing the code rate progressively to the values 2/3, 3/4 while keeping the constellation size fixed to 64-QAM. The gain in communication robustness provided by the use of more channel coding exceeds the loss in communication

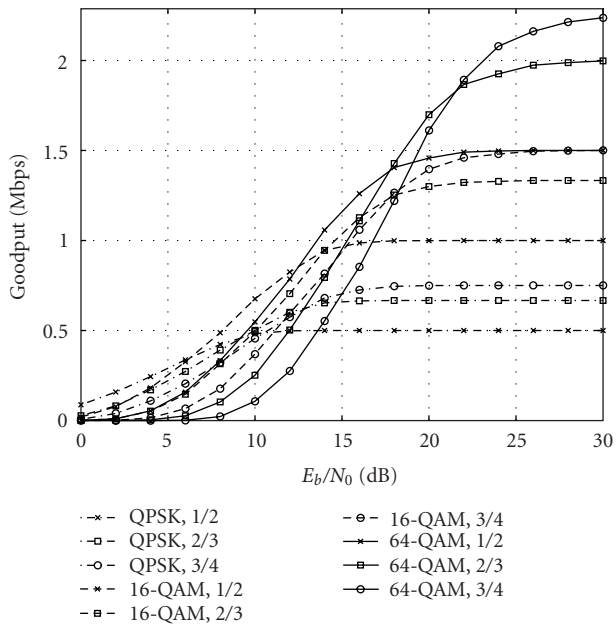

Figure 5: Tradeoff between channel coding rate and constellation, static downlink, MCBS-CDMA, using MRC.

robustness due to the use of a higher constellation. As it will be shown later, the conclusion may be reversed in a mobile environment due to better robustness of lower-order mappings to changing channel conditions.

Figures 6 and 7 illustrate the gain obtained by the use of different multiple-antenna techniques in the downlink of an MCBS-CDMA-based static system and in the uplink of an SCBS-CDMA-based static system, respectively. Four different system configurations are considered ($1\times1, 1\times2, 2\times1, 2\times2$). A typical user's load is assumed (number of users equal to 5). Two optimal combinations of the constellation and channel coding rate are considered (16-QAM with coding rate 1/2, 64-QAM with coding rate 3/4). Exploiting the spatial diversity at the mobile terminal or at the base station by the use of two antennas (1×2 or 2×1 configurations), MRC reception, or STBC transmission enables a significant gain in transmit power (up to 12 dB gain is achieved in the downlink, up to 7 dB gain is achieved in the uplink). However, the additional gain obtained by combining STBC transmission with MRC reception (2×2 configuration) is relatively small (less than 2 dB). SDM suffers from a high 8 dB loss in the goodput regions that can also be reached by a single-antenna system (this loss can be reduced if more complex nonlinear receivers are considered). One can only achieve an increase of capacity by the use of multiple antennas at very high signal-to-noise ratio (SNR) values. As a result, we advise to use one directive antenna at the base station to exploit the very small angle spread and increase the cell capacity, and two diversity antennas at the mobile terminal to improve the link reliability. The receive MRC technique is performed in the downlink, while the STBC coding scheme is applied in the uplink.

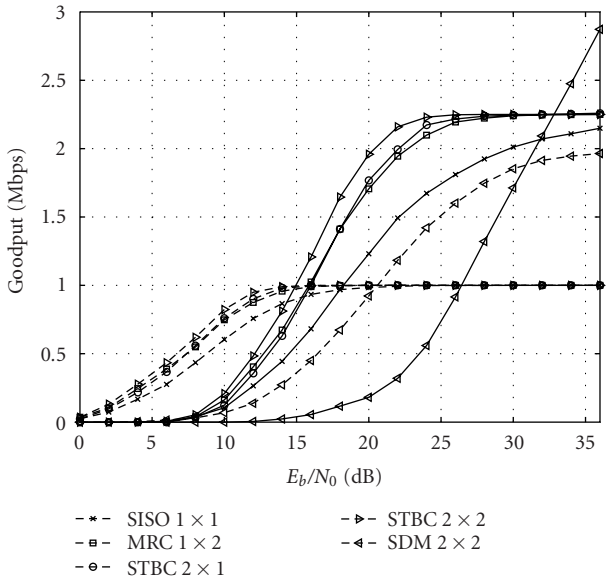

Figure 6: Multiple-antenna gain in the downlink, static environment, MCBS-CDMA; dashed curves: 16-QAM and coding rate 1/2, solid curves: 64-QAM and coding rate 3/4.

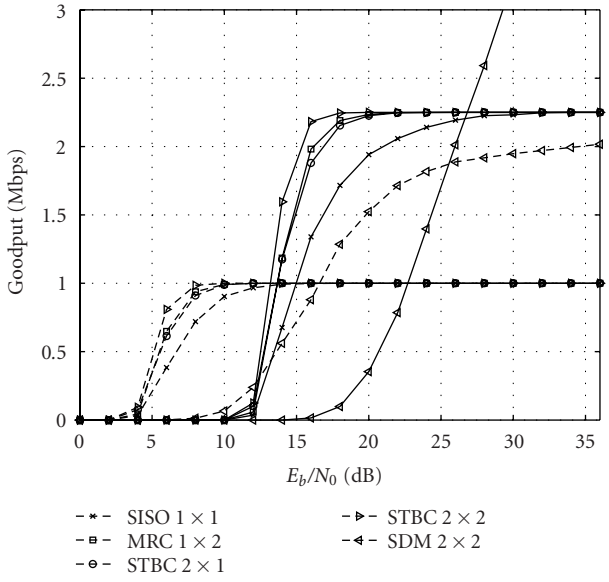

Figure 7: Multiple-antenna gain in the uplink, static environment, SCBS-CDMA; dashed curves: 16-QAM and coding rate 1/2, solid curves: 64-QAM and coding rate 3/4.

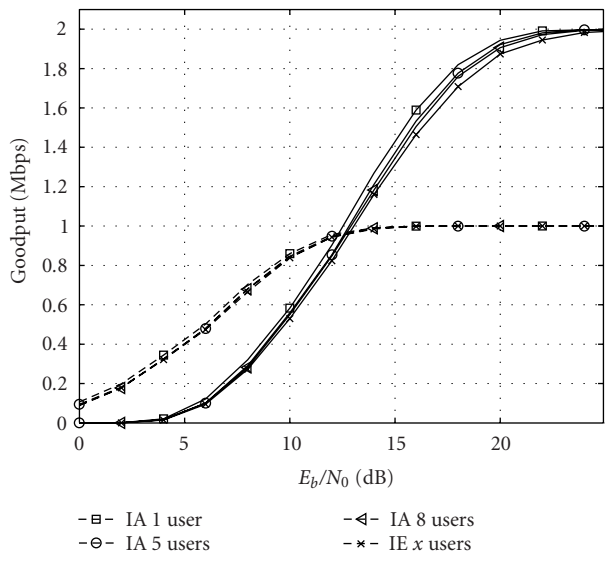

Figure 8: Impact of the user load on the downlink, static environment, MCBS-CDMA (IE stands for interblock spreading) and MC-CDMA (IA stands for intrablock spreading), using MRC; dashed curves: 16-QAM and coding rate 1/2, solid curves: 64-QAM and coding rate 3/4.

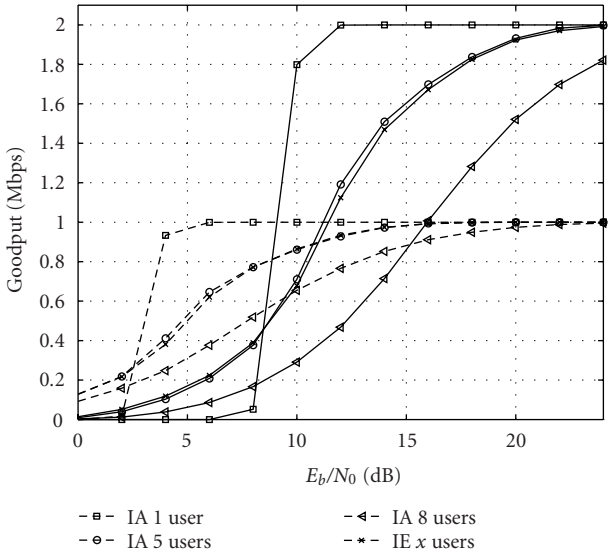

Figure 9: Impact of the user load on the uplink, static environment, SCBS-CDMA (IE stands for interblock spreading) and SC-CDMA (IA stands for intrablock spreading), using STBC; dashed curves: 16-QAM and coding rate 1/2, solid curves: 64-QAM and coding rate 3/4.

Figures 8 and 9 illustrate the system performance sensitivity to the user's load assuming static channels. Interblock spreading (MCBS-CDMA and SCBS-CDMA) is compared to intrablock spreading (MC-CDMA and SC-CDMA). The number of users ranges from 1 to 8. Again the same two combinations of the constellation and channel coding rate have been selected (16-QAM with coding rate 1/2, 64-QAM with coding rate 3/4). In case of interblock spreading, the MMSE multiuser receiver reduces to an equivalent but simpler single-user receiver, which performs channel-independent block despreading followed by MMSE single-user equalization. MCBS-CDMA and SCBS-CDMA are MUI-free transmission schemes, such that their user's goodput remains unaffected by the user's load. In case of intrablock spreading, the MMSE multiuser receiver outperforms the single-user detector. In the downlink, the performance of the MMSE multiuser joint detector is slightly decreasing for an increasing number of users and converges to the one of the

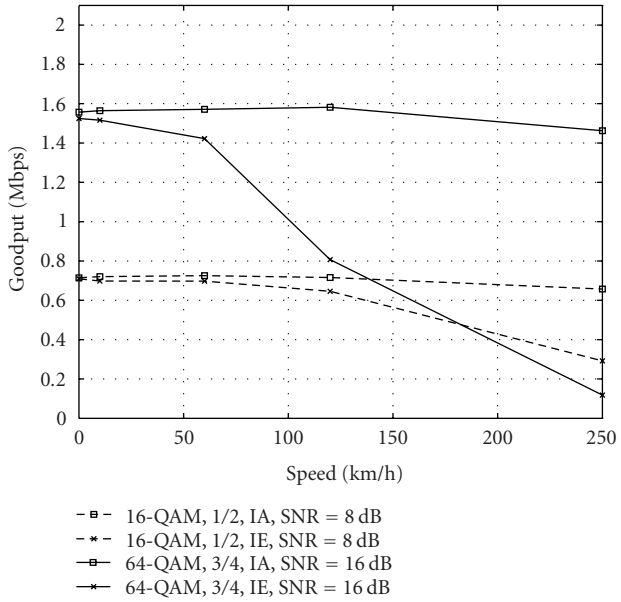

Figure 10: Impact of the terminal speed on the downlink, MCBS-CDMA (IE stands for interblock spreading) and MC-CDMA (IA stands for intrablock spreading), using MRC.

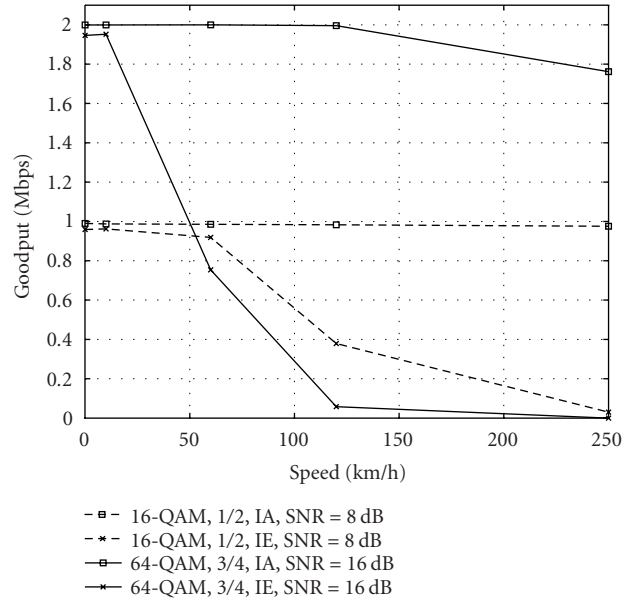

Figure 11: Impact of the terminal speed on the uplink, SCBS-CDMA (IE stands for interblock spreading) and SC-CDMA (IA stands for intrablock spreading), using STBC.

single-detector at full user load. MMSE multiuser reception is especially needed in the uplink, since a single-user receiver cannot get rid of the MUI, and features a BER curve flattening already at low SNRs. The impact of the user's load is much more pronounced in the SC-CDMA uplink than in the MC-CDMA downlink since the signals propagate through different channels, which is more difficult to compensate for. In the downlink, MC-CDMA always outperforms MCBS-CDMA since it benefits from the frequency diversity offered by the CDMA spreading. In the uplink, the performance of SCBS-CDMA is equivalent to the one of SC-CDMA for a typical user's load, worse for a small user's load and better for a high user's load.

Figures 10 and 11 compare the effect of the terminal speed on the user's goodput in case of intrablock and interblock spreading. A typical user's load of 5 users has been assumed, which makes MC-CDMA (SC-CDMA) and MCBS-CDMA (SCBS-CDMA) perform equally well in static conditions. For each combination of the constellation and coding rate, the SNR value corresponding to the maximum slope in the goodput curves has been chosen (realistic working point in the curves illustrated in Figures 8 and 9). Since the symbol block duration is higher in case of interblock spreading than in case of intrablock spreading, the performance of MCBS-CDMA (SCBS-CDMA) is significantly reduced, while the performance of MC-CDMA (SC-CDMA) remains acceptable when the speed of the mobile terminals increases. Since the orthogonality between the users is lost when the speed increases, the impact is more severe in the uplink than in the downlink. If a 10-percent performance loss is acceptable, interblock spreading should be used up to 60 km/h in the downlink or 10 km/h in the uplink for detection complexity reasons, while intrablock spreading should be used for higher speeds. This conclusion is in line with the two-dimensional spreading strategy proposed in [16, 17] for a MC-based system, that prioritizes the spreading in the time domain rather than in the frequency domain, for the sake of complexity and performance. It is also interesting to note that the goodput achieved with high constellations at high speed is smaller than the goodput achieved with low constellations.

6. CONCLUSIONS

A generic transmission scheme has been designed that allows to instantiate all the combinations of OFDM and cyclic-prefixed SC modulations with DS-CDMA. The SDM and STBC multiple-antenna techniques have been integrated in the generic transmission scheme. For each resulting mode, the optimal linear MMSE multiuser receiver has been derived.

A mode selection strategy has also been proposed that trades off efficiently the communication performance in a typical suburban dynamic outdoor environment with the complexity and PAPR at the mobile terminal.

(i) A hybrid modulation scheme (MC in the downlink, SC in the uplink) should be used in order to minimize the mobile terminal PAPR and data processing power.

(ii) Under low-to-medium mobility conditions, it is better to use a high constellation and a low channel coding rate to achieve the maximum goodput for a given SNR value. However, the lowest constellation order should be selected under high mobility conditions.

(iii) One directive antenna should be used at the base station to increase the cell capacity and multiple antennas should be used at the mobile terminal in combination with

diversity techniques like MRC reception and STBC transmission to improve the link reliability.

(iv) Since interblock and intrablock spreading perform equally well in typical user loads, interblock spreading should be used at low terminal speeds to minimize the data processing complexity while intrablock spreading should only be used at high terminal speeds.

It has been demonstrated that an adaptive transceiver is interesting to support different communication modes and to efficiently track the changing communication conditions.

REFERENCES

[1] T. Ojanperä and R. Prasad, *Wideband CDMA for Third Generation Mobile Communications*, Artech House, Norwood, Mass, USA, 1998.

[2] R. van Nee, G. Awater, M. Morikura, H. Takanashi, M. Webster, and K. W. Halford, "New high-rate wireless LAN standards," *IEEE Commun. Mag.*, vol. 37, no. 12, pp. 82–88, 1999.

[3] D. Falconer, S. L. Ariyavisitakul, A. Benyamin-Seeyar, and B. Eidson, "Frequency domain equalization for single-carrier broadband wireless systems," *IEEE Commun. Mag.*, vol. 40, no. 4, pp. 58–66, 2002.

[4] N. Yee, J.-P. Linnartz, and G. Fettweis, "Multicarrier CDMA in indoor wireless radio networks," in *Proc. IEEE International Symposium on Personal, Indoor and Mobile Radio Communications (PIMRC '93)*, vol. 1, pp. 109–113, Yokohama, Japan, September 1993.

[5] K. Fazel, "Performance of CDMA/OFDM for mobile communication system," in *Proc. 2nd IEEE International Conference on Universal Personal Communications (ICUPC '93)*, vol. 2, pp. 975–979, Ottawa, Ontario, Canada, October 1993.

[6] K. Fazel, S. Kaiser, and M. Schnell, "A flexible and high performance cellular mobile communications system based on multi-carrier SSMA," *Kluwer Journal of Wireless Personal Communications*, vol. 2, no. 1/2, pp. 121–144, 1995.

[7] S. Kaiser, "OFDM code-division multiplexing in fading channels," *IEEE Trans. Commun.*, vol. 50, no. 8, pp. 1266–1273, 2002.

[8] V. M. DaSilva and E. S. Sousa, "Multicarrier orthogonal CDMA signals for quasi-synchronous communication systems," *IEEE J. Select. Areas Commun.*, vol. 12, no. 5, pp. 842–852, 1994.

[9] S. Kondo and L. B. Milstein, "Performance of multicarrier DS-CDMA systems," *IEEE Trans. Commun.*, vol. 44, no. 2, pp. 238–246, 1996.

[10] L.-L. Yang and L. Hanzo, "Multicarrier DS-CDMA: a multiple access scheme for ubiquitous broadband wireless communications," *IEEE Commun. Mag.*, vol. 41, no. 10, pp. 116–124, 2003.

[11] F. Petré, G. Leus, M. Moonen, and H. De Man, "Multicarrier block-spread CDMA for broadband cellular downlink," *EURASIP Journal on Applied Signal Processing*, vol. 2004, no. 10, pp. 1568–1584, 2004, *Special Issue on Multi-Carrier Communications and Signal Processing* .

[12] M. Vollmer, M. Haardt, and J. Gotze, "Comparative study of joint-detection techniques for TD-CDMA based mobile radio systems," *IEEE J. Select. Areas Commun.*, vol. 19, no. 8, pp. 1461–1475, 2001.

[13] K. L. Baum, T. A. Thomas, F. W. Vook, and V. Nangia, "Cyclic-prefix CDMA: an improved transmission method for broadband DS-CDMA cellular systems," in *Proc. IEEE Wireless Communications and Networking Conference (WCNC '02)*, vol. 1, pp. 183–188, Orlando, Fla, USA, March 2002.

[14] S. Zhou, G. B. Giannakis, and C. Le Martret, "Chip-interleaved block-spread code division multiple access," *IEEE Trans. Commun.*, vol. 50, no. 2, pp. 235–248, 2002.

[15] F. Petré, G. Leus, L. Deneire, and M. Moonen, "Downlink frequency-domain chip equalization for single-carrier block transmission DS-CDMA with known symbol padding," in *Proc. IEEE Global Telecommunications Conference (GLOBECOM '02)*, vol. 1, pp. 453–457, Taipei, Taiwan, November 2002.

[16] H. Atarashi, N. Maeda, S. Abeta, and M. Sawahashi, "Broadband packet wireless access based on VSF-OFCDM and MC/DS-CDMA," in *Proc. 13th IEEE International Symposium on Personal, Indoor and Mobile Radio Communications (PIMRC '02)*, vol. 3, pp. 992–997, Lisbon, Portugal, September 2002.

[17] N. Chapalain, D. Mottier, and D. Castelain, "An OFCDM uplink transmission system with channel estimation based on spread pilots," in *Proc. IST Mobile and Wireless Communications Summit*, Lyon, France, June 2004.

[18] G. J. Foschini and M. J. Gans, "On limits of wireless communications in a fading environment when using multiple antennas," *Kluwer Journal of Wireless Personal Communications*, vol. 6, no. 3, pp. 311–335, 1998.

[19] G. G. Raleigh and J. M. Cioffi, "Spatio-temporal coding for wireless communication," *IEEE Trans. Commun.*, vol. 46, no. 3, pp. 357–366, 1998.

[20] D. Gesbert, H. Bolcskei, D. A. Gore, and A. J. Paulraj, "Outdoor MIMO wireless channels: models and performance prediction," *IEEE Trans. Commun.*, vol. 50, no. 12, pp. 1926–1934, 2002.

[21] A. J. Paulraj and T. Kailath, "Increasing capacity in wireless broadcast systems using distributed transmission/directional reception (DTDR)," U.S. Patent 5345599, Stanford University, Stanford, Calif, USA, 1994.

[22] G. J. Foschini, "Layered space-time architecture for wireless communication in a fading environment when using multiple antennas," *Bell Labs Technical Journal*, vol. 1, no. 2, pp. 41–59, 1996.

[23] F. W. Vook, T. A. Thomas, and K. L. Baum, "Transmit array processing for cyclic-prefix CDMA," in *Proc. 56th IEEE Vehicular Technology Conference (VTC '02)*, vol. 1, pp. 270–274, Vancouver, British Columbia, Canada, September 2002.

[24] V. Tarokh, N. Seshadri, and A. R. Calderbank, "Space-time codes for high data rate wireless communication: performance criterion and code construction," *IEEE Trans. Inform. Theory*, vol. 44, no. 2, pp. 744–765, 1998.

[25] S. M. Alamouti, "A simple transmit diversity technique for wireless communications," *IEEE J. Select. Areas Commun.*, vol. 16, no. 8, pp. 1451–1458, 1998.

[26] V. Tarokh, H. Jafarkhani, and A. R. Calderbank, "Space-time block codes from orthogonal designs," *IEEE Trans. Inform. Theory*, vol. 45, no. 5, pp. 1456–1467, 1999.

[27] E. Lindskog and A. J. Paulraj, "A transmit diversity scheme for channels with intersymbol interference," in *Proc. IEEE International Conference on Communications (ICC '00)*, vol. 1, pp. 307–311, New Orleans, La, USA, June 2000.

[28] N. Al-Dhahir, "Single-carrier frequency-domain equalization for space-time block-coded transmissions over frequency-selective fading channels," *IEEE Commun. Lett.*, vol. 5, no. 7, pp. 304–306, 2001.

[29] S. Zhou and G. B. Giannakis, "Single-carrier space-time block-coded transmissions over frequency-selective fading channels," *IEEE Trans. Inform. Theory*, vol. 49, no. 1, pp. 164–179, 2003.

[30] S. Barbarossa and F. Cerquetti, "Simple space-time coded

SS-CDMA systems capable of perfect MUI/ISI elimination," *IEEE Commun. Lett.*, vol. 5, no. 12, pp. 471–473, 2001.
[31] F. W. Vook, T. A. Thomas, and K. L. Baum, "Cyclic-prefix CDMA with antenna diversity," in *Proc. 55th IEEE Vehicular Technology Conference (VTC '02)*, vol. 2, pp. 1002–1006, Birmingham, Ala, USA, May 2002.
[32] F. Petré, G. Leus, L. Deneire, M. Engels, M. Moonen, and H. De Man, "Space-time block coding for single-carrier block transmission DS-CDMA downlink," *IEEE J. Select. Areas Commun.*, vol. 21, no. 3, pp. 350–361, 2003, *Special Issue on MIMO Systems and Applications* .
[33] Z. Liu and G. B. Giannakis, "Space-time block-coded multiple access through frequency-selective fading channels," *IEEE Trans. Commun.*, vol. 49, no. 6, pp. 1033–1044, 2001.
[34] A. Stamoulis, Z. liu, and G. B. Giannakis, "Space-time block-coded OFDMA with linear precoding for multirate services," *IEEE Trans. Signal Processing*, vol. 50, no. 1, pp. 119–129, 2002.
[35] Z. Wang and G. B. Giannakis, "Wireless multicarrier communications," *IEEE Signal Processing Mag.*, vol. 17, no. 3, pp. 29–48, 2000.
[36] G. B. Giannakis, P. A. Anghel, and Z. Wang, "Wideband generalized multicarrier CDMA over frequency-selective wireless channels," in *Proc. IEEE Int. Conf. Acoustics, Speech, Signal Processing (ICASSP '00)*, vol. 5, pp. 2501–2504, Istanbul, Turkey, June 2000.
[37] G. B. Giannakis, Z. Wang, A. Scaglione, and S. Barbarossa, "AMOUR-generalized multicarrier transceivers for blind CDMA regardless of multipath," *IEEE Trans. Commun.*, vol. 48, no. 12, pp. 2064–2076, 2000.
[38] Q. Chen, E. S. Sousa, and S. Pasupathy, "Performance of a coded multi-carrier DS-CDMA system in multipath fading channels," *Kluwer Journal of Wireless Personal Communications*, vol. 2, no. 1-2, pp. 167–183, 1995.
[39] A. Klein, G. K. Kaleh, and P. W. Baier, "Zero forcing and minimum mean-square-error equalization for multiuser detection in code-division multiple-access channels," *IEEE Trans. Veh. Technol.*, vol. 45, no. 2, pp. 276–287, 1996.
[40] L. Vandendorpe, "Performance analysis of IIR and FIR linear and decision-feedback MIMO equalizers for transmultiplexers," in *Proc. IEEE International Conference on Communications (ICC '97)*, vol. 2, pp. 657–661, Montreal, Quebec, Canada, June 1997.
[41] 3GPP Technical specification group, "TR25.996 v6.1.0, Spatial channel model for Multiple Input Multiple Output (MIMO) simulations," September 2003.

François Horlin was born in Bruxelles, Belgium, in 1975. He received the Electrical Engineering degree and the Ph.D. degree from the Université catholique de Louvain (UCL), Louvain-la-Neuve, Belgium, in 1998 and 2002, respectively. In September 2002, he joined the Interuniversity Micro-Electronics Center (IMEC), Leuven, Belgium, as a Senior Researcher. He is currently the Head of the research activities on digital signal processing for broadband communications. His fields of interest are in digital signal processing, mainly for high-bit-rate multiuser communications. During his Ph.D. thesis, he proposed a new solution for jointly optimizing the transmitter and the receiver in a multiuser multi-input multi-output (MIMO) type of communication systems. He is now working on the integration of a multistandard mobile terminal. In this context, he is responsible for the development of the functionality of a fourth-generation (4G) cellular system, targeting high capacity in very high mobility conditions.

Frederik Petré was born in Tienen, Belgium, on December 12, 1974. He received the Electrical Engineering degree and the Ph.D. degree in applied sciences from the Katholieke Universiteit Leuven (KULeuven), Leuven, Belgium, in July 1997 and December 2003, respectively. In September 1997, he joined the Design Technology for Integrated Information and Communication Systems (DESICS) Division at the Interuniversity Micro-Electronics Center (IMEC) in Leuven, Belgium. Within the Digital Broadband Terminals (DBATE) Group of DESICS, he first performed predoctoral research on wireline transceiver design for twisted pair, coaxial cable, and powerline communications. During the fall of 1998, he visited the Information Systems Laboratory (ISL) at Stanford University, Calif, USA, working on OFDM-based powerline communications. In January 1999, he joined the Wireless Systems (WISE) Group of DESICS as a Ph.D. researcher, funded by the Institute for Scientific and Technological Research in Flanders (IWT). Since January 2004, he has been a Senior Scientist within the Wireless Research Group of DESICS. He is investigating the baseband signal processing algorithms and architectures for future wireless communication systems, like third-generation (3G) and fourth-generation (4G) cellular networks, and wireless local area networks (WLANs). His main research interests are in modulation theory, multiple-access schemes, channel estimation and equalization, smart antenna, and MIMO techniques. He is a Member of the ProRISC Technical Program Committee and the IEEE Benelux Section on Communications and Vehicular Technology (CVT). He is a Member of the Executive Board and Project Leader of the Flexible Radio Project of the Network of Excellence in Wireless Communications (NEWCOM), established under the sixth framework of the European Commission.

Eduardo Lopez-Estraviz was born in Ferrol, Spain, in 1977. He received the Telecommunications Engineering degree from the Universidad de Vigo (UVI), Vigo, Spain, in 1996 and 2002, respectively. In June 2002, he joined the Interuniversity Micro-Electronics Center (IMEC), Leuven, Belgium, as a researcher. His fields of interest are in digital signal processing for broadband communications. He is now working on the integration of a multistandard mobile terminal. In this context, he is working on developing functionality for a fourth-generation (4G) cellular system, targeting high capacity in very high mobility conditions.

Frederik Naessens was born in Roeselare, Belgium, in 1979. He received the Engineering degree from the Catholic School for Higher Education Bruges-Ostend (KHBO) Academy in Ostend, Belgium, in 2001. After this studies, he joined the Interuniversity Micro-Electronics Center (IMEC), Leuven, Belgium, as a development engineer. Currently he is also a part-time student following an M.S. degree in ICT at the University of Kent, United Kingdom. He has been involved in a demonstrator setup for GPS and GLONASS satellite navigation systems. He is now working on developing functionality for future cellular systems (4G).

Liesbet Van der Perre received the M.S. degree and the Ph.D. degree in electrical engineering from the KU Leuven, Belgium, in 1992 and 1997, respectively. Her work in the past focused on system design and digital modems for high-speed wireless communications. She was a System Architect in IMEC's OFDM ASICs development and a Project Leader for the turbo codec. Currently, she is leading the Software-Defined Radio Baseband Project, and she is the Scientific Director of Wireless Research in IMEC.